Journal of Solid State Chemistry 182 (2009) 1913–1920

Contents lists available at ScienceDirect

Journal of Solid State Chemistry

journal homepage: www.elsevier.com/locate/jssc

Two new hydrogen bond-supported supramolecular compounds assembly from tungsten–vanadium polyoxoanions and copper complex fragments

Ji-Wen Cui [a,b], Yan Chen [a], Xiao-Bing Cui [a,*], Hai-Hui Yu [a,c], Jia-Ning Xu [a], Ji-Qing Xu [a,*], Wei-Jie Duan [a], Tie-Gang Wang [a]

[a] *College of Chemistry and State Key Laboratory of Inorganic Synthesis and Preparative Chemistry, Jilin University, Changchun 130021, PR China*
[b] *College of Chemistry and Pharmacy, Jiamusi University, Jiamusi 154000, PR China*
[c] *College of Chemical Engineering, NorthEast Dianli University, Jiamusi 132000, PR China*

ARTICLE INFO

Article history:
Received 5 February 2009
Received in revised form
20 April 2009
Accepted 26 April 2009
Available online 10 May 2009

Keywords:
Tungsten–vanadium polyoxoanion
Hydrothermal synthesis
Bi-supported keggin
Tetranuclear complex cation clusters
Supramolecular compounds

ABSTRACT

Two new supramolecular compounds based on tungsten–vanadium polyoxoanions formulated as $[Cu(2,2'\text{-bipy})_3]_2H_{14}[PW_{2.2}V_{9.8}O_{40}(VO)_2[Cu(2,2'\text{-bipy})_2H_2O]_2][PW_{2.2}V_{9.8}O_{40}(VO)_2]\cdot 10H_2O$ (**1**) and $[Cu_4(2,2'\text{-bipy})_4(H_2O)_2(PO_4)_2]H_{6.5}[PW_{8.4}V_{3.6}O_{40}]\cdot 2H_2O$ (**2**) (2,2′-bipy = 2,2′-bipyridine) have been synthesized hydrothermally and characterized by IR, TG, XPS and X-ray diffraction analyses. Crystal structure analyses reveal that compounds **1** and **2** exhibit novel 2D supramolecular layer structures constructed from tungsten–vanadium polyoxoanions and different types of secondary building units (SBUs), respectively, the different SBUs are formed by $[Cu(2,2'\text{-bipy})_2H_2O]^{2+}$ and $[Cu(2,2'\text{-bipy})_3]^{2+}$ cations in compound **1** and $[Cu_4(2,2'\text{-bipy})_4(H_2O)_2(PO_4)_2]^{2+}$ cations in **2**, respectively. Study of magnetic properties indicated the presence of antiferromagnetic behaviors for both compound **1** and **2**.

1. Introduction

Over the past decades, supramolecular chemistry has become a very interesting focus of investigation by several research groups [1]. This expansion has been driven by the growing knowledge regarding synthetic and characterization methods for complex structures [2–4]. The directed assembly of supramolecular arrays from discrete molecular building blocks is a topic of significant interest with potential applications in the areas of catalysis, molecular electronics, sensor design, and optics [5–10]. In the construction of supramolecular materials, one important strategy is that those of low-dimensional building blocks extend to high-dimensional networks through weak intermolecular interactions, including hydrogen-bonding, $\pi\ldots\pi$ stacking and weak van der Waals interactions, etc. Doubtless, the hydrogen bond play a major role in supramolecular assembles by virtue of its unique strength and directionality that may control short-range packing [11].

Chemistry of polyoxometalates (POMs) has been investigated intensively for reasons of both fundamental and applied significance [12–18], especially, the Keggin POMs have been successfully exploited [19–30]. However, supramolecular compounds based on POMs have been unexplored in past decades, though the spherical surfaces of the POMs give a better opportunity in forming hydrogen bonds with the organic/inorganic moieties. In recent years, extensive efforts have been focused on the design and assembly of such kind of supramolecular architectures and a few high-dimensional supramolecular architectures have been synthesized [31–33].

The nucleophilic characteristic of the POMs allows specific assembly with electrophilic fragments and it is expected to produce supramolecular materials via hydrogen-bonding interactions. Taking into account of this, a motivation for design and synthesis of supramolecular compounds containing POMs and organic amines has been put forward. A prominent subclass of POMs is the family of tungsten–vanadium clusters, to the best of our knowledge, the vanadium-containing POMs present a wide range interesting topologies and structures, as a continuous effort to the class of tungsten–vanadium clusters [34], we recently have focused on the use of W–V clusters as structural building blocks in the syntheses of hydrogen-bonded high-dimensional structures, for such assembly system has not been explored thoroughly. In this paper, we report the syntheses and characterizations of two new supramolecular compounds based on tungsten–vanadium polyoxoanion formulated as $[Cu(2,2'\text{-bipy})_3]_2H_{14}[PW_{2.2}V_{9.8}O_{40}(VO)_2[Cu(2,2'\text{-bipy})_2H_2O]_2][PW_{2.2}V_{9.8}O_{40}(VO)_2]\cdot 10H_2O$ (**1**), which contains the first tungsten–vanadium heteropolyoxoanion where the content of V is higher than that of W, and $[Cu_4(2,2'\text{-bipy})_4(H_2O)_2(PO_4)_2]H_{6.5}[PW_{8.4}V_{3.6}O_{40}]\cdot 2H_2O$ (**2**) which is the first example of 1D chain structure based on the Keggin

---

* Corresponding authors. Fax: +86 431 85168624.
E-mail addresses: cuixb@mail.jlu.edu.cn (X.-B. Cui), xjq@mail.jlu.edu.cn (J.-Q. Xu).

0022-4596/$ - see front matter © 2009 Elsevier Inc. All rights reserved.
doi:10.1016/j.jssc.2009.04.037

tungsten–vanadium polyoxoanions linked by tetranuclear cations. Each of them exhibits a novel 2D supramolecular layer structures based on tungsten-vanadium clusters. In this work, based on the same organic groups (2,2′-bipy) in compounds **1** and **2**, their different hydrogen-bonding interactions and molecular arrays have been discussed due to their different POMs. The synthesis of the two organic–inorganic hybrid materials may not only provide hybrid compounds, but also advance the understanding of hybrid material.

2. Experimental section

2.1. Materials and measurements

All reagents used were purchased and used without further purification. The elemental analyses (C, H and N) were performed on a Perkin-Elmer 2400 CHN elemental analyzer. The elemental analyses (P, W and V) were performed on a Perkin-Elmer Optima 3300DV spectrophotometer. The infrared spectra were recorded with a Perkin-Elmer SPECTRUM ONE FTIR spectrophotometer with a KBr pellet in the 4000–400 cm^{-1} region. XPS analyses were performed on a VG ESCALAB MK II spectrometer with an Mg$K\alpha$ (1253.6 eV) achromatic X-ray source. The thermogravimetric analyses (TGA) were carried out on a Perkin-Elmer TAG-7000 instrument from room temperature to 800 °C, with a heating rate of 10 °C/min under atmosphere. Magnetic susceptibility (χ) measurements were carried out using a Quantum Design MPMS-7 SQUID Magnetometer. Data were collected over 4–300 K at 1000 G, using 43.1 and 69.0 mg masses, respectively.

2.2. Preparation

2.2.1. Preparation of $[\mathrm{Cu(2,2'\text{-}bipy)_3}]_2\mathrm{H_{14}\{PW_{2.2}V_{9.8}O_{40}(VO)_2[Cu(2,2'\text{-}bipy)_2H_2O]_2\}\ [PW_{2.2}V_{9.8}O_{40}(VO)_2]\cdot 10H_2O}$ ***(1)***

Compound **1** was hydrothermally synthesized in 68% yield (based on V). A mixture of $\mathrm{Na_2WO_4\cdot 2H_2O}$ (0.60 g), $\mathrm{V_2O_5}$ (0.33 g), $\mathrm{CuAc_2\cdot H_2O}$ (0.60 g), 2,2′-bipy (0.09 g), $\mathrm{H_3PO_4}$ (0.9 mL) and $\mathrm{H_2O}$ (20 mL) was necessarily adjusted to pH = 7.5. The resultant mixture was sealed in a 25 mL Teflon-lined autoclave and heated at 180 °C for 96 h. After being cooled to room temperature, the red–brown block crystals were obtained. Elem. anal: $\mathrm{C_{100}H_{118}N_{20}Cu_4P_2W_{4.4}V_{23.6}O_{96}}$: calcd: C, 21.97%; H, 2.18%; N, 5.14%; P, 1.14%; W, 14.83%; V, 22.02%. Found: C, 22.34%; H, 2.22%; N, 5.23%; P, 1.11%; W, 14.43%; V, 21.56%. IR (cm^{-1}): 1604(s), 1566(w), 1500(m), 1469(s), 1449(vs), 1318(s), 1247(s), 1172(s), 1106(s), 1062(s), 1032(s), 965(w), 939(vs), 871(m), 767(vs), 725(m), 645(m), 588(m), 510(m) and 376(m).

2.2.2. Preparation of $[\mathrm{Cu_4(2,2'\text{-}bipy)_4(H_2O)_2(PO_4)_2}]\mathrm{H_{6.5}[PW_{8.4}V_{3.6}O_{40}]\cdot 2H_2O}$ ***(2)***

Compound **2** was hydrothermally synthesized in 38% yield (based on W). A mixture of $\mathrm{WO_3}$(1.12 g), $\mathrm{NH_4VO_3}$ (0.56 g), $\mathrm{CuSO_4\cdot 5H_2O}$ (0.60 g), 2,2′-bipy (0.18 g) and $\mathrm{H_2O}$ (20 mL) was necessarily adjusted to pH = 4. The resultant mixture was sealed in a 25 mL Teflon-lined autoclave and heated at 180 °C for 96 h. After being cooled to room temperature, the black block single crystals were obtained. Elem. anal: $\mathrm{C_{40}H_{46.5}N_8Cu_4P_3W_{8.4}V_{3.6}O_{52}}$: calcd: C, 13.55%; H, 1.32%; N, 3.16%; P, 2.62%; W, 43.55%; V, 5.17%. Found: C, 13.81%; H, 1.34%; N, 3.22%; P, 2.56%; W, 42.65%; V, 5.08%. IR (cm^{-1}): 1602(s), 1566(w), 1497(m), 1473(s), 1445(vs), 1315(s), 1249(s), 1162(m), 1127(m), 1074(s), 1052(m), 1032(s), 965(vs), 882(vs), 813(vs), 765(s), 729(s), 594(m), 505(m) and 386(s).

2.3. X-ray crystallography

The structures of compounds **1** and **2** were determined by single-crystal X-ray diffraction analyses. A red–brown block shaped crystal of **1** and a black block shaped crystal of **2** were glued on a glass fiber, respectively. The data of compounds **1** and **2** were collected on a Rigaku R-AXIS RAPID IP diffractometer and a Siemens SMART CCD diffractometer with Mo$K\alpha$ radiation ($\lambda = 0.71073$ Å) at 293 K in the range of $3.01^\circ < \theta < 27.48^\circ$ and in the range of $2.37^\circ < \theta < 26.11^\circ$, respectively. The empirical absorption corrections of the compounds were applied. The structures were solved by direct methods and refined by the full-matrix least squares based on F^2 using the SHELXTL Version 5.1 software package. All of the non-hydrogen atoms except the O5W and O6W of compound **1** were refined anisotropically. The positions of the hydrogen atoms attached to carbon atoms were fixed at their ideal positions, and those attached to oxygen atoms were not located. *Crystal data for* **1***:* triclinic, space group *P*-1, $R(\mathrm{int}) = 0.0335$, $a = 12.926(3)$ Å, $b = 13.884(3)$ Å, $c = 24.396(5)$ Å, $\alpha = 86.50(3)^\circ$, $\beta = 82.71(3)^\circ$, $\gamma = 63.36(3)^\circ$, $Z = 2$, $V = 3881.8(14)$ Å^{-3}. A total of 37 525 reflections were measured. Structure solution and refinements based on 17 313 independent reflections and 1167 parameters gave $R_1(\omega R_2) = 0.0628$ (0.1501). *Crystal data for* **2***:* triclinic, space group *P*-1, $R(\mathrm{int}) = 0.0471$, $a = 12.060(2)$ Å, $b = 12.085(2)$ Å, $c = 13.581(3)$ Å, $\alpha = 109.32(3)^\circ$, $\beta = 103.04(3)^\circ$, $\gamma = 90.94(3)^\circ$, $Z = 1$, $V = 1810.8(6)$ Å^{-3}. A total of 15 241 reflections were measured. Structure solution and refinements based on 7018 independent reflections and 563 parameters gave $R_1(\omega R_2) = 0.0507$ (0.1145).

3. Results and discussion

3.1. Synthesis discussion

Compounds **1** and **2** were synthesized under different conditions. We have carefully explored the reactivity of the P/W/V/Cu system under hydrothermal conditions. The starting materials ($\mathrm{Na_2WO_4\cdot 2H_2O}$ or $\mathrm{WO_3}$, $\mathrm{V_2O_5}$ or $\mathrm{NH_4VO_3}$ and $\mathrm{CuAc_2\cdot H_2O}$ or $\mathrm{CuSO_4\cdot 5H_2O}$) were varied as well as the initial pH value of the mixtures, while the organic ligand 2,2′-bipy and distilled water were left unchanged. Two different crystalline compounds have been isolated. The pH of the solution plays an important role in the isolation of the two compounds. Only when pH is 7.5 or higher, we succeeded in synthesizing the compound **1**, while when pH is 4–6, we succeeded in synthesizing the compound **2**. In order to improve the yield of the compound **2**, we have done many parallel experiments by changing the amount of starting materials and the initial pH value. Unfortunately, we did not achieve this goal. With the same molar ratio of $\mathrm{WO_3/NH_4VO_3}$/2,2′-bipy, only $\mathrm{CuSO_4\cdot 5H_2O}$ was replaced by the $\mathrm{NiAc_2\cdot 4H_2O}$, we obtained another compound in 70% yield (based on W) [34]. The $\mathrm{H_3PO_4}$ not only is a starting material but also adjusts the pH value of the reaction mixture in synthesizing the compound **2**. 2, 2′-bipy plays the double roles of coordination ligand and reductant in preparation of compounds **1** and **2**. The syntheses of the compounds **1** and **2** are shown in Scheme 1.

3.2. Crystal structure of compound ***1***

The single crystal X-ray diffraction analysis reveals that the asymmetric unit of compound **1** contains two $[\mathrm{PW_{2.2}V_{9.8}O_{40}(VO)_2}]^{11-}$ anions. As shown in Fig. 1, the $[\mathrm{PW_{2.2}V_{9.8}O_{40}(VO)_2}]^{11-}$ anion (POM **1**) is a derivative of the pseudo-Keggin anion $[\mathrm{P}M_{12}\mathrm{O_{40}}]^{17-}$ (M represents the disordered W and V). The anion

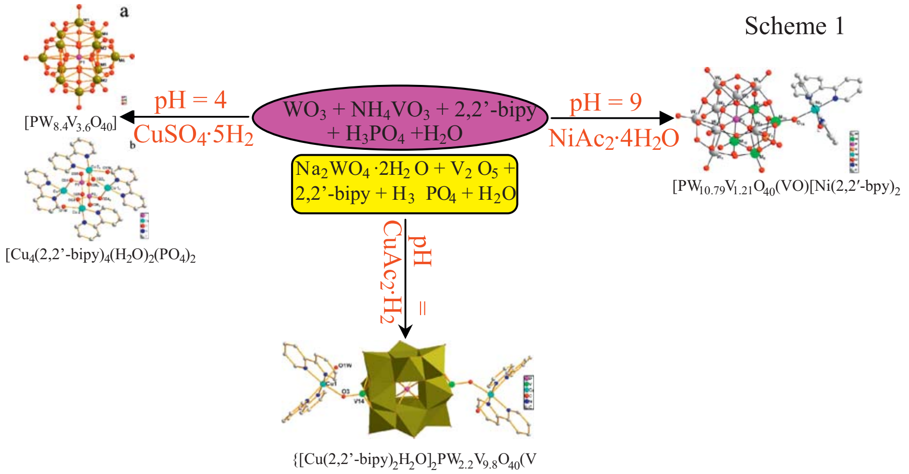

Scheme 1.

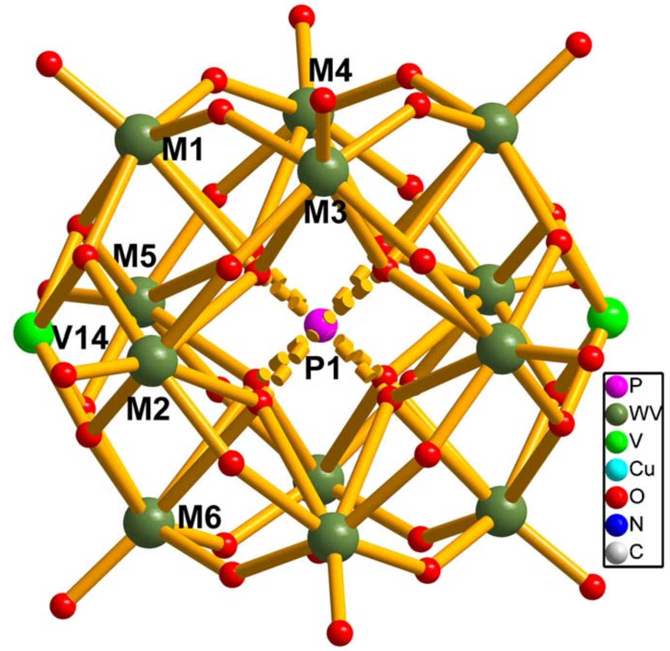

Fig. 1. View of the structure of the bi-capped polyoxoanion of **1**.

$[PM_{12}O_{40}]^{17-}$ is composed of a disordered PO_4 tetrahedron surrounded by four vertex-sharing M_3O_{13} triads which result from the association of three edge-sharing MO_6 octahedra. In the MO_6 octahedra, the position of M_1 is crystallographically disordered with occupancies of 0.167 and 0.833 for W and V, M_2 is 0.223 and 0.777, M_3 is 0.138 and 0.862, M_4 is 0.156 and 0.844, M_5 is 0.184 and 0.816 and M_6 is 0.227 and 0.773, respectively. The contents of W and V revealed by X-ray analysis are consistent with the results from elemental analyses. M centers exhibit MO_6 octahedral coordination environments with M-O_t (terminal oxygen atoms) distances ranging from 1.612(6) to 1.630(6) Å, M-O_b (bridging oxygen atoms) distances ranging from 1.776(7) to 2.060(6) Å and M-O_a (central oxygen atoms) distances ranging from 2.335(9) to 2.528(8) Å. The nucleophilic pseudo-Keggin derivative $[PW_{2.2}V_{9.8}O_{40}]^{17-}$ in POM **1** is then capped by two $[VO]^{3+}$ ions to form a bi-capped cluster POM **1**. The V atom (V14) of $[VO]^{3+}$ ion bonds to one terminal oxygen atom and four triply bridging oxygen atoms in a distorted pyramidal arrangement. The V-O_t (terminal oxygen atom) bond length is 1.635(5) Å, and V-O_{3b} (tri-bridging oxygen atoms) bond lengths are in the range of 1.839(7)–1.921(5) Å. The central P atom is located at the inversion center, which results in a disordered PO_4 tetrahedron, that is, the central P atom is surrounded by a cube of eight oxygen atoms with each oxygen site half-occupied. The P–O distances range from 1.425(8) to 1.624(8) Å.

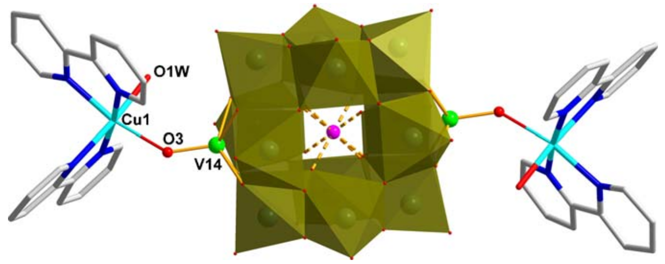

Fig. 2. View of the structure of the bi-capped polyoxoanion bisupported TMC of **1**. All hydrogen atoms are omitted for clarity.

In addition, the other anionic moiety of compound **1** is the $[PW_{2.2}V_{9.8}O_{40}(VO)_2]^{11-}$ anion (POM **2**). The shell structure of POM **2** is very similar to that of the POM **1**. The P–O, W–O and V–O bond lengths are comparable with those in POM **1**. In the MO_6 octahedra, the position of M_7 is crystallographically disordered with occupancies of 0.167 and 0. 833 for W and V, M_8 is 0.228 and 0.772, M_9 is 0.185 and 0.815, M_{10} is 0.130 and 0.870, M_{11} is 0.158 and 0.842 and M_{12} is 0.208 and 0.792, respectively. Selected bond lengths of POM **1** and POM **2** are listed in Table S1. The bond valence sum calculations [35] are 6.38–6.54 for the W atoms and 4.53–4.64 for the V atoms (except 4.71–4.84 for the capping V13 and V14) in POM **1** and POM **2**. According to the bond valence sum calculations, charge balance requirements and elemental analyses, the POM **1** and POM **2** are formulated as $[PW^{VI}_{2.2}V^{V}_{5.7}V^{IV}_{4.1}O_{40}(V^{V}O)_2]^{11-}$, in agreement with the XPS spectrum analysis. The location of the hydrogen atoms in a new anion has been a difficult question, as ever stated by Patterson [36].

The biggest difference between POM **1** and POM **2** is that the POM **1** of compound **1** is covalently bonded to two cations $[Cu(2,2'\text{-bipy})_2H_2O]^{2+}$ through terminal oxygen atoms (O3 and its symmetry equivalent) of two opposite capping V atoms (V14 and its symmetry equivalent). Therefore, two terminal cations $[Cu(2,2'\text{-bipy})_2H_2O]^{2+}$ link two V–O terminal groups of the polyoxoanion to generate a novel bi-capped tungsten–vanadium polyoxoanion bi-supported transition metal complex (TMC) $\{[Cu(2,2'\text{-bipy})_2H_2O]_2PW_{2.2}V_{9.8}O_{40}(VO)_2\}^{7-}$, which is the first example of bi-supported Keggin-type tungstovanadophosphate (see Fig. 2). The POM **2** is a discrete anion.

The $[PW_{2.2}V_{9.8}O_{40}(VO)_2]^{11-}$ anion of compound **1** is the first heteropolyoxoanion where the content of V is higher than that of W. To now, Keggin-type monometallic polyoxoanions based on tungsten ($[XW_{12}O_{40}]^{n-}$) have formed one of the biggest families of POMs [37]. However, about the Keggin-type monometallic polyoxoanions based on vanadium, to our knowledge, the POMs containing $[XV_{12}O_{40}]^{n-}$ are only present in $[PV_{14}O_{42}]^{9-}$ [38], $[VV_{14}O_{36}(OH)_6]^{6-}$ [39] and $[H_{12}V_{12}O_{36}(VO_4)]^{4-}$ [40]. It is very interesting to compare the number of Keggin-type vanadates with that of the Keggin-type tungstates. The sparsity of Keggin-type vanadates might come from the reason that a high negative charge will prevent the formation of the Keggin anion $[XV_{12}O_{40}]^{15-}$. Recently, several examples of Keggin-type mixed metallic POMs based on tungsten-vanadium have been successfully isolated, such as $[(V^{V}O_4)W^{VI}_{8}M_4(V^{IV}O)_2]^{n-}$ ($M = 0.71V^{IV}+0.29W^{VI}$, $n = 4.68$) [41]; $[PW_9V_3O_{40}]^{6-}$ [42]; $[PW_{11}VO_{40}]^{4-}$ [43]; $[W_{10}V_5O_{42}]^{4-}$ [44]; $[PW_9V_3O_{40}(VO)_2]^{5-}$ [45] and $[PW_9V_3O_{40}(VO)_3]^{8-}$ [46]; in all those mixed tungsten–vanadium polyoxoanions, the content of V is lower than that of W, perhaps attributing to the lower negative charge of the tungsten–vanadium polyoxoanions (W:V > 1) than that of the polyoxoanions (W:V<1), so the stabilization of the former is higher than that of the latter. Heretofore, the tungsten–vanadium polyoxoanion with the Keggin structures where the content of V is higher than that of W has not been reported. The $[PW_{2.2}V_{9.8}O_{40}(VO)_2]^{11-}$ anion of compound **1** is the first heteropolyoxoanion where the content of V is higher than that of W.

The bi-capped polyoxoanion bisupported TMC $\{[Cu(2,2'\text{-bipy})_2H_2O]_2PW_{2.2}V_{9.8}O_{40}(VO)_2\}^{7-}$ connects each other through hydrogen-bonding interactions forming an infinite 1D supramolecular chain (chain A) $\{[Cu(2,2'\text{-bipy})_2H_2O]_2PW_{2.2}V_{9.8}O_{40}(VO)_2\}_n^{7n-}$ along the *b*-axis with a corresponding O1W···O6W (and its symmetry equivalents) distance of 2.919 Å and O6W···O6$_a$ (and its symmetry equivalents) distance of 3.006 Å. The adjacent clusters of POM **2** connect each other through hydrogen-bonding interactions with O3W···O35 (and its symmetry equivalents) distance of 2.915 Å, along with O3W···O34$_a$ (and its symmetry equivalents) distance of 3.148 Å, resulting in an infinite 1D supramolecular chain (chain B) $\{PW_{2.2}V_{9.8}O_{40}(VO)_2\}_n^{11n-}$. Chains A and B alternate to give birth to a 2D supramolecular framework through hydrogen-bonding interactions with O5W$_a$···O6W$_a$ (and its symmetry equivalents) distance of 2.696 Å, O2W···O5W$_a$ (and its symmetry equivalents) distance of 2.806 Å, as well as O2W···O25 (and its symmetry equivalents) distance of 3.080 Å (see Fig. 3). The synergetic effects have strengthened the stability of the supramolecular structure of compound **1**. To our knowledge, this is the first example of this kind of structure.

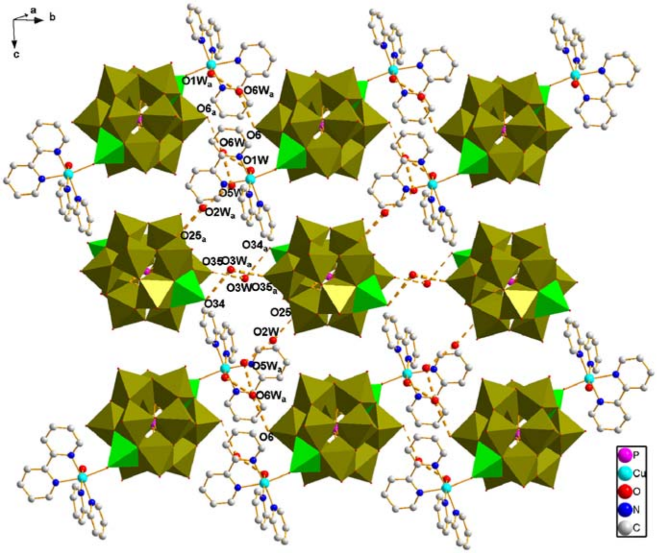

Fig. 3. The structure of compound **1** showing a novel supramolecular layers structure. All hydrogen atoms are omitted for clarity. Symmetry codes for the generated equivalent atoms: a: $-x$, $-y$, $-z$.

3.3. Crystal structure of compound 2

As shown in Fig. 4a, the tungsten–vanadium polyoxoanion $[PW_{8.4}V_{3.6}O_{40}]^{8.5-}$ of compound **2** exhibits a pseudo-Keggin structure, which is similar to that in the compound **1**. The difference is that the polyoxoanion of **2** is the heteropolyoxoanion where the content of W is higher than that of V, while the polyoxoanion of **1** is the first heteropolyoxoanion where the content of V is higher than that of W. The P–O, W–O and V–O bond lengths are comparable with those in compound **1**. In the MO_6 octahedra, the position of M_1 is crystallographically disordered with occupancies of 0.771 and 0. 229 for W and V, M_2 is 0.619 and 0.381, M_3 is 0.649 and 0.351, M_4 is 0.682 and 0.318, M_5 is 0.755 and 0.245 and M_6 is 0.705 and 0.295, respectively. The contents of W and V revealed by X-ray analysis are consistent with the result from elemental analysis. Selected bond lengths of **2** are listed in Table S2. The bond valence sum calculations [35] are 6.30–6.47 for the W atoms and 4.47–4.60 for the V atoms in **2**, indicating the polyoxoanion of **2** to be formulated as $[PW^{VI}_{8.4}V^{V}_{1.8}V^{IV}_{1.8}O_{40}]^{8.5-}$, in agreement with the XPS spectrum analysis.

An unusual feature of **2** is the structure of the tetranuclear complex cation cluster $[Cu_4(2,2'\text{-bipy})_4(H_2O)_2(PO_4)_2]^{2+}$. Fig. 4b shows the structure of the tetranuclear complex cation cluster and the coordination environments of the coppers and phosphorus atoms. The cationic cluster consists of two central $[PO_4]^{3-}$ tetrahedra, corner-sharing with four $[CuO_3N_2]^{2+}$ distorted square pyramids. The $[CuO_3N_2]^{2+}$ coordination geometry of the two Cu1 centers is defined by two nitrogen donors from a 2,2′-bipy ligand [Cu1–N 1.991(10)–2.014(10) Å], an oxygen donor from one $[PO_4]^{3-}$ tetrahedron (O24 of P2 group) [Cu1–O24 1.916(8) Å], a μ_3-oxo donor from the other $[PO_4]^{3-}$ tetrahedron (O23 of P2$_a$ group) [Cu1–O23 1.950(8) Å] and an oxygen donor of the water molecule (O1W) [Cu1–O1W 2.619(9) Å]. One of the three oxygen donors (O1W) has a significantly longer distance than that of the other two oxygen donors from the two different $[PO_4]^{3-}$ tetrahedra (O23 and O24) for the reason of the John-Teller effect. The two Cu (Cu1 and Cu1$_a$), two P (P2 and P2$_a$) and four oxygen atoms form a novel eight-atom ring. The $[CuO_3N_2]^{2+}$ coordination geometry of the two Cu2 centers is coordinated by two nitrogen donors from a 2,2′-bipy ligand [Cu2–N 1.989(9)–1.990(10) Å], an oxygen donor from one $[PO_4]^{3-}$ tetrahedron (O25 of P2 group) [Cu2–O25 1.914(8) Å], a μ_3-oxo donor from the other $[PO_4]^{3-}$ tetrahedron (O23 of P2$_a$ group) [Cu2–O23 2.314(9) Å] and an oxygen donor of the water molecule (O1W) [Cu2–O1W 2.129(8) Å]. In addition, the P–O distances in cation $[Cu_4(2,2'\text{-bipy})_4(H_2O)_2(PO_4)_2]^{2+}$ are between 1.512(9) and 1.581(8) Å.

The most unsual feature of comopund **2** is that tungsten–vanadium polyoxoanions $[PW_{8.4}V_{3.6}O_{40}]^{8.5-}$ are linked to the tetranuclear cations $[Cu_4(2,2'\text{-bipy})_4(H_2O)_2(PO_4)_2]^{2+}$ to form a 1D chain. Each polyoxoanion $[PW_{8.4}V_{3.6}O_{40}]^{8.5-}$ is weak covalently bonded to two cations $[Cu_4(2,2'\text{-bipy})_4(H_2O)_2(PO_4)_2]^{2+}$ through terminal oxygen atoms (O5 and its symmetry equivalent) of two opposite W atoms [Cu2–O5 and Cu2$_a$–O5$_a$ 2.938 Å], alternatively, each cation $[Cu_4(2,2'\text{-bipy})_4(H_2O)_2(PO_4)_2]^{2+}$ is linked to two tungsten-vanadium polyoxoanions $[PW_{8.4}V_{3.6}O_{40}]^{8.5-}$ to form the 1D chain. Additionally, the cation $[Cu_4(2,2'\text{-bipy})_4(H_2O)_2(PO_4)_2]^{2+}$ was exactly deposited between two polyoxoanions,

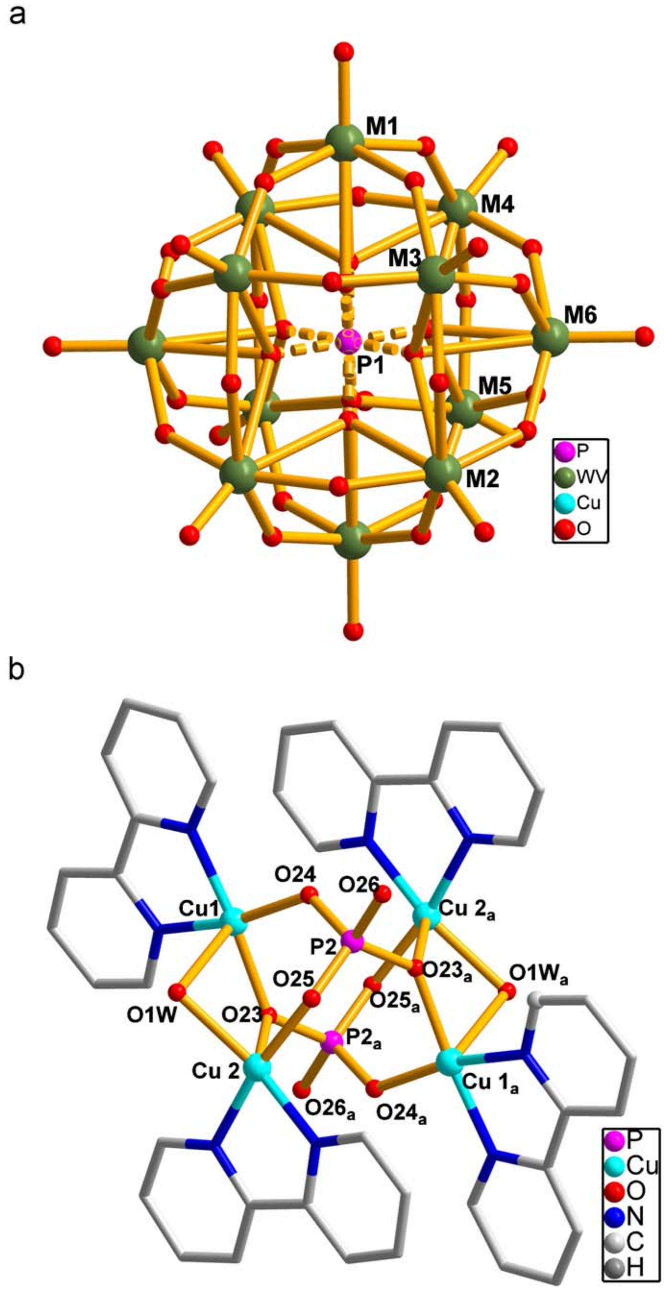

Fig. 4. View of the structure of the (a) $[PW_{8.4}V_{3.6}O_{40}]^{8.5-}$ polyoxoanion and (b) $[Cu_4(2,2'\text{-bipy})_4(H_2O)_2(PO_4)_2]^{2+}$ cation of **2**. All hydrogen atoms are omitted for clarity. Symmetry codes for the generated equivalent atoms: a: $-x$, $-y$, $-z$.

and links the two anions via extra hydrogen bonds with O1W···O11 (and its symmetry equivalents) distance of 3.069 Å. The synergetic effects have strengthened the stability of the 1D chain structure of compound **2**. The 1D chain connects each other through hydrogen-bonding interactions forming an infinite 2D supramolecular framework with O2W···O4$_a$ (and its symmetry equivalents) distance of 2.907 Å, O2W···O4 (and its symmetry equivalents) distance of 3.092 Å, as well as O1W···O8 (and its symmetry equivalents) distance of 2.704 Å, shown in Fig. 5.

To date, only a few compounds incorporating POMs with tetranuclear cations were synthesized [45,47–51]. such as compound $[Co_4(HPO_3)_2(C_{12}H_8N_2)_8(H_2O)_2](H_3O)[PW_9V_3O_{40}(VO)_2]$ where tetranuclear cation $[Co_4(HPO_3)_2(C_{12}H_8N_2)_8(H_2O)_2]^{4+}$ only serves as the balanced cation [45] and compound $[Co_4(phen)_8(H_2O)_2(HPO_3)_2](H_3O)_3[PMo_8V_4O_{40}(VO)_2]$ which shows a 2D supramolecular network constructed by the linking of tetranuclear cations and POMs via hydrogen bonds [50]. Only one example where tetranuclear cation $[Cu_4(terpy)_4(PO_4)(H_2O)_2]^{5+}$ is covalently bonded to polyoxoanion $[PW_{12}O_{40}]^{5-}$ to form extended structure was reported [51]. To our knowledge, the 1D chain structure of compound **2** is the first example which is based on the tungsten–vanadium mixed metallic polyoxoanions linked by tetranuclear cations. Both the building units and the linked mode between the 1D chain structure reported in literature 51 and that of compound **2** are quite different.

3.4. *XPS spectra*

The XPS spectrum of compound **1** (Fig. 6a) gives two overlapped peaks at 517.2 and 516.3 eV, attributable to V^{5+} $2p_{3/2}$ and V^{4+} $2p_{3/2}$, respectively. The XPS spectrum of compound **2** (Fig. 6b) gives two overlapped peaks at 517.9 and 516.7 eV, attributable to V^{5+} $2p_{3/2}$ and V^{4+} $2p_{3/2}$, respectively. These results further confirm the oxidation state of V atoms in compounds **1** and **2**.

3.5. *TG analysis*

The TG analysis curve of compound **1** (Fig. 7a) can be divided into two steps of weight loss in the range of 85–635 °C. The first weight loss of 3.83% occurs in the temperature range 85–360 °C, corresponding to the removal of two coordinated water molecules and ten-crystal water molecules (Calcd. 3.95%). The second weight loss 29.87% starts at 360 °C up to 635 °C with the calculated value of 28.85% is attributed to ten 2,2′-bipyridine ligands. The whole weight loss (33.70%) is in good agreement with the calculated value (32.8%). Compound **1** gains weight at temperatures higher than 635 °C is attributed to the oxidation of the V^{IV}.

The TG curve of compound **2** (Fig. 7b) is also divided into two stages. The first weight loss is 1.80% in the temperature range 100–350 °C, corresponding to the release of two coordinated water molecule and two-crystal water molecule (Calcd. 2.04%). The second weight loss of 17.51% from 350 to 560 °C is attributed to the disappearing of four 2,2′-bipyridine ligands (Calcd. 17.68%). The total weight loss (19.31%) is in good agreement with the calculated value (19.83%). Compound **2** gains weight at temperatures higher than 700 °C is attributed to the oxidation of the V^{IV}.

3.6. *Magnetic properties*

The magnetic susceptibility (χ) measurement of compounds **1** and **2** were collected with a Quantum Design MPMS-7 SQUID Magnetometer. Preliminary magnetic studies have been performed on powder samples of **1** and **2** in the range of 4–300 K. The susceptibility of **1** and **2** were corrected for diamagnetism. Fig. 8 shows the magnetic behaviour of **1** in forms of μ_{eff} vs. T plot and χ_m^{-1} vs. T plot (insert). The effective magnetic moment (μ_{eff}) at 300 K is 8.27μ_B. Upon cooling, the μ_{eff} continuously decreases to a minimum value of 2.59μ_B at 4 K, indicating the presence of the antiferromagnetic exchange interactions. The magnetic data of sample **1** obey the Curie–Weiss law in the range 100–300 K, and give values $C = 19.802$ emu mol^{-1} K and $\theta = -398.043$ K, characteristic of the antiferromagnetic interactions of **1**. The magnetic behavior of **2** is similar to that of compound **1**, which is shown in Fig. 9 in the forms of μ_{eff} vs. T and χ_m^{-1} vs. T plots. The effective magnetic moment (μ_{eff}) at 300 K is 3.44μ_B. Upon cooling, the μ_{eff} continuously decreases to a minimum value of 2.49μ_B at 4 K, indicating the presence of the antiferromagnetic exchange interactions. There is a certain degree of deviation from the Curie–Weiss law, especially at high temperature, for the plots of

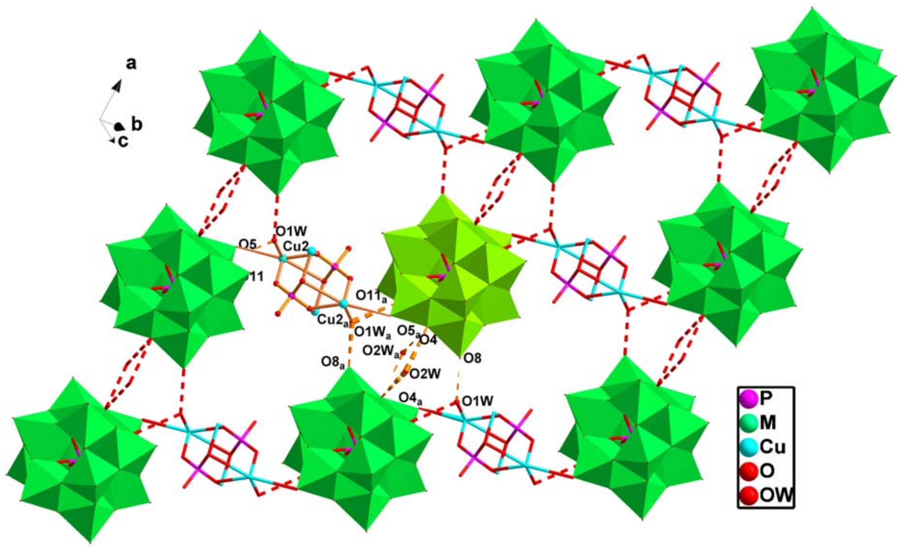

Fig. 5. The structure of compound **2** showing a novel supramolecular layers structure. All hydrogen atoms are omitted for clarity. Symmetry codes for the generated equivalent atoms: a: −*x*, −*y*, −*z*.

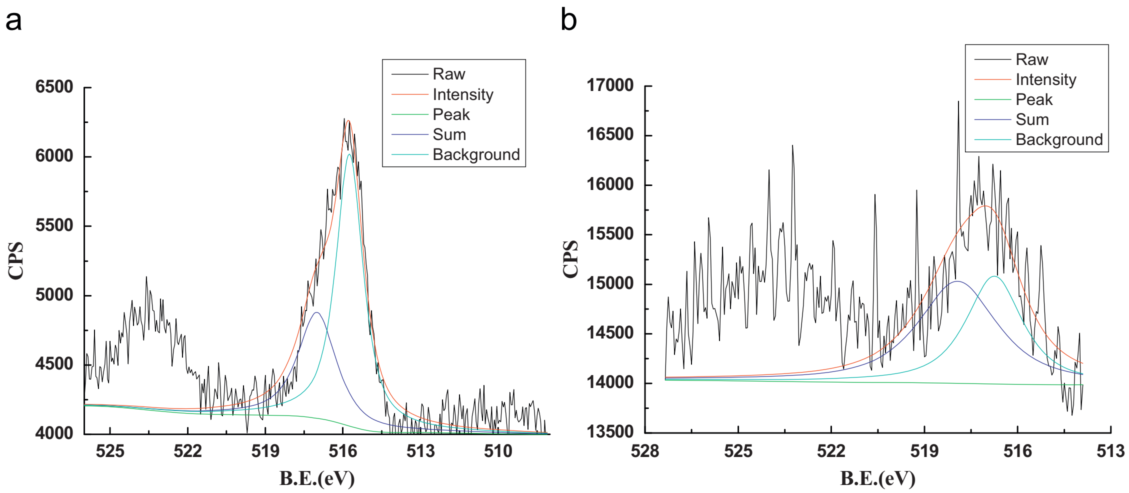

Fig. 6. (a) The XPS spectrum of compound **1** and (b) the XPS spectrum of compound **2**.

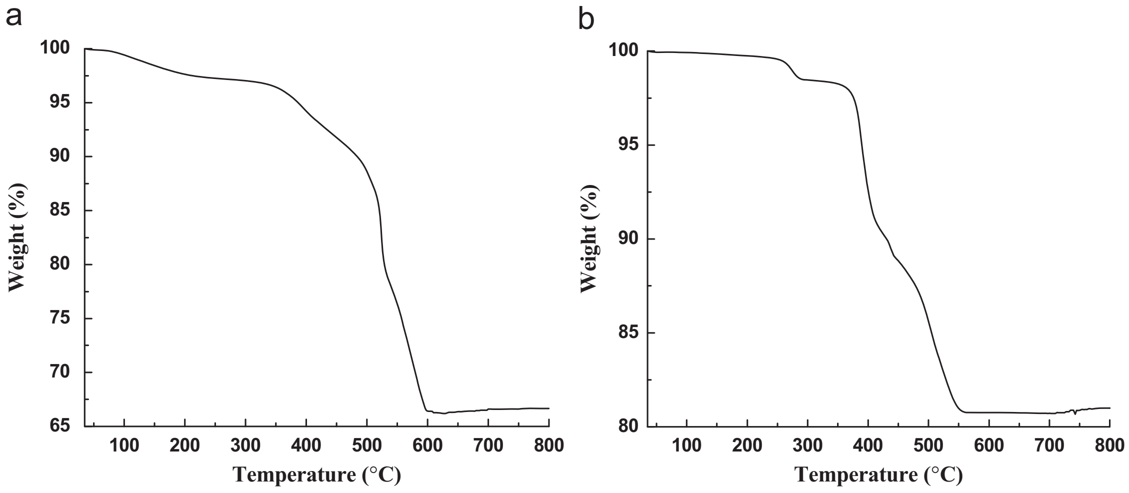

Fig. 7. (a) TG curve of compound **1** and (b) TG curve of compound **2**.

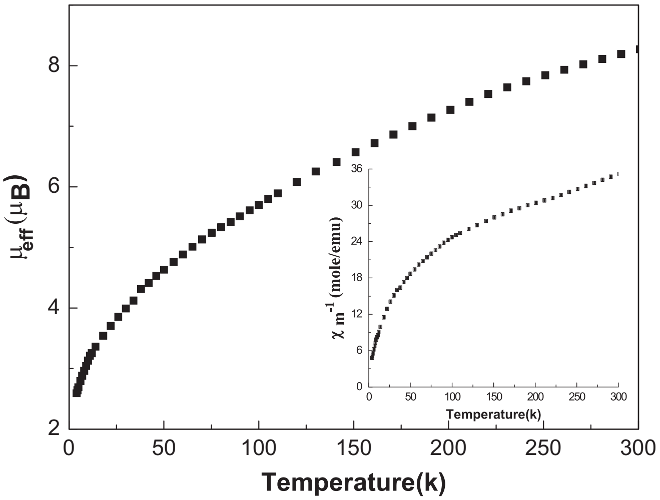

Fig. 8. The effective magnetic moment, μ_{eff} for compound **1** on the temperature, *T*. Insert: The dependence of the reverse susceptibilities, χ_m^{-1} on the temperature, *T*.

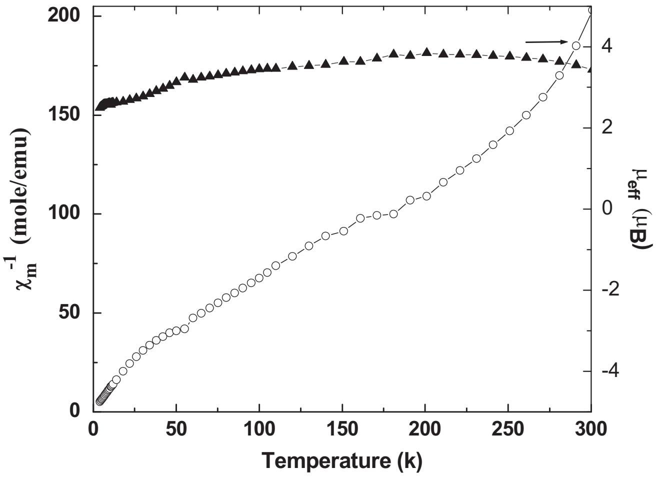

Fig. 9. The dependence of the reverse susceptibilities, χ_m^{-1} and the effective magnetic moment, μ_{eff} for compounds **2** on the temperature, *T*.

χ_m^{-1} of compound **2**, which is probably caused by the impurity of the test samples. However, the existing data are in line with the Curie–Weiss law Basically in the range of 55–250 K which can show that the magnetic characteristics of compound **2**, and give values $C = 2.138\,\text{emu}\,\text{mol}^{-1}\,\text{K}$ and $\theta = -42.920\,\text{K}$, characteristic of the antiferromagnetic interactions of **2**.

4. Conclusions

In summary, two new hydrogen-bonded high-dimensional supramolecular architectures have been synthesized and structurally characterized. Compound **1** contains the first tungsten-vanadium polyoxoanion where the content of V is higher than that of W. Compound **2** is the first example of 1D chain structure, which is based on the Keggin tungsten–vanadium polyoxoanions linked by tetranuclear complex cation clusters. Study of magnetic properties indicated the presence of antiferromagnetic behaviour for compounds **1** and **2**. Extended researches are underway to reveal the synthetic rules and explore their attractive properties.

Supporting information

Crystallograhpic data for the structural analysis have been deposited with the Cambridge Crystallgraphic Data Center, CCDC reference numbers 673263 and 689911, respectively. These data can be obtained free of charge at www.ccdc.cam.ac.uk/contas/retrieving.html (or from the Cambridge Crystallographic Data Center, 12, Union Road, Cambridge CB21EZ, UK. Phone: +44-(0) 1223/336-408; fax: +44-(0) 1223/336-033. E-mail: deposit@ccdc.cam.ac.uk).

Acknowledgments

This work was financially supported by the National Natural Science Foundation of China (nos. 20571032 and 20333070).

Appendix A. Supplementary data

Supplementar data associated with this article can be found in the online version at doi:10.1016/j.jssc.2009.04.037.

References

[1] D. Braga, L. Maini, F. Grepioni, Chem. Eur. J. 8 (2002) 1804.
[2] F. Vogtle, Supramolecular Chemistry, Wiley, Chichester, 1991.
[3] J.M. Lehn, Supramolecular Chemistry, VCH, New York, 1995.
[4] J.M. Lehn, Comprehensive Supramolecular Chemistry, Pergamon, New York, 1996.
[5] J.M. Lehn, Angew Chem. Int. Ed. Engl. 29 (1990) 1304.
[6] J.M. Lehn, Supramolecular Chemistry, VCH, Weinheim, 1995.
[7] C.N.R. Rao, S. Natarajan, R. Vaidhyanathan, Angew. Chem. Int. Ed. 43 (2004) 1466.
[8] O.M. Yaghi, M. O'Keeffe, N.W. Ockwig, H.K. Chae, M. Eddaoudi, J. Kim, Nature 423 (2003) 705.
[9] B.F. Abrahams, A. Hawley, M.G. Haywood, T.A. Hudson, R. Robson, D.A. Slizys, J. Am. Chem. Soc. 126 (2004) 2894.
[10] J.L.C. Rowsell, O.M. Yaghi, Microporous Mesoporous. Mater. 73 (2004) 3.
[11] S.V. Kolotuchin, E.E. Fenlon, S.R. Wilson, C.J. Loweth, S.C. Zimmerman, Angew. Chem. Int. Ed. 34 (1995) 2654.
[12] A. Müller, M. Koop, P. Schiffels, H. Bögge, Chem. Commun. (1997) 1715.
[13] Y. Xu, H.G. Zhu, H. Cai, X.Z. You, Chem. Commun. (1999) 787.
[14] Y. Xu, D.R. Zhu, Z.J. Guo, Y.J. Shi, K.L. Zhang, X.Z. You, J. Chem. Soc. Dalton Trans. (2001) 772.
[15] E. Burkholder, J. Zubieta, Chem. Commun. (2001) 2056.
[16] C.M. Liu, S. Gao, H.M. Hu, Z.M. Wang, Chem. Commun. (2001) 1636.
[17] R.C. Finn, J. Zubieta, Inorg. Chem. 40 (2001) 2466.
[18] C.D. Wu, C.Z. Lu, H.H. Zhuang, J.S. Huang, Inorg. Chem. 41 (2002) 5636.
[19] M. Cindrič, B. Kamenar, N. Strukan, Z. Veksli, Polyhedron 14 (1995) 1045.
[20] P.J. Zapf, C.J. Warren, R.C. Haushalter, J. Zubieta, Chem. Commun. (1997) 1543.
[21] D. Hagrman, P.J. Zapf, J. Zubieta, Chem. Commun. (1998) 1283.
[22] Y. Xu, J.Q. Xu, K.L. Zhang, Y. Zhang, X.Z. You, Chem. Commun. (2000) 153.
[23] B. Yan, Y. Xu, X. Bu, N.K. Goh, L.S. Chia, G.D. Stucky, J. Chem. Soc. Dalton Trans. 8 (2001) 2009.
[24] W. Yang, C. Lu, H.J. Zhuang, J. Chem. Soc. Dalton Trans. (2002) 2879.
[25] Y.P. Ren, X.J. Kong, X.Y. Hu, M. Sun, L.S. Long, R.B. Huang, L.S. Zheng, Inorg. Chem. 45 (2006) 4016.
[26] M.I. Khan, S. Cevik, R. Hayashi, J. Chem. Soc. Dalton Trans. (1999) 1651.
[27] C.M. Liu, D.Q. Zhang, M. Xiong, D.B. Zhu, Chem. Commun. (2002) 1416.
[28] L.J. Zhang, X.L. Zhao, J.Q. Xu, T.G. Wang, J. Chem. Soc. Dalton Trans. (2002) 3275.
[29] M. Yuan, Y.G. Li, E.B. Wang, C.G. Tian, L. Wang, C.W. Hu, N.H. Hu, H.Q. Jia, Inorg. Chem. 42 (2003) 3670.
[30] C.M. Liu, D.Q. Zhang, D.B. Zhu, Cryst. Growth Des. 6 (2006) 524.
[31] H. Kumagai, M. Arishima, S. Kitagawa, K. Ymada, S. Kawata, S. Kaizaki, Inorg. Chem. 41 (2002) 1989.
[32] C. Streb, D.L. Long, L. Cronin, Cryst. Eng. Commun. 8 (2006) 629.
[33] V. Coué, R. Dessapt, M. Bujoli-Doeuff, M. Evain, S. Jobic, Inorg. Chem. 46 (2007) 2824.
[34] J.W. Cui, X.B. Cui, H.H. Yu, J.Q. Xu, Z.H. Yi, W.J. Duan, Inorg. Chim. Acta 361 (2008) 2641.
[35] I.D. Brown, in: M. O'Keefe, A. Navrotsky (Eds.), Structure and Bonding in Crystals, vol. 2, Academic Press, New York, 1981, p. 1.
[36] L. Pettersson, I. Andersson, O.W. Howarth, Inorg. Chem. 31 (1992) 4032.
[37] M.T. Pope, Heteropoly and Isopoly Oxometalates, Springer, New York, 1983.
[38] R. Kato, A. Kobayashi, Y. Sasaki, Inorg. Chem. 21 (1982) 240.
[39] T. Duraisamy, N. Ojha, A. Ramanan, J.J. Vittal, Chem. Mater. 11 (1999) 2339.

[40] N. Hao, C. Qin, Y. Xu, E.B. Wang, Y.G. Li, E.H. Shen, L. Xu, Inorg. Chem. Commun. 8 (2005) 592.

[41] V. Shivaiah, S. Hajeebu, S.K. Das, Inorg. Chem. Commun. 5 (2002) 996.

[42] G.Y. Luan, Y.G. Li, S.T. Wang, E.B. Wang, Z.B. Han, C.W. Hu, N.H. Hu, H.Q. Jia, J. Chem. Soc. Dalton Trans. (2003) 233.

[43] L. Lisnard, A. Dolbecq, P. Mialane, J. Marrot, E. Rivière, S.A. Borshch, S. Petit, V. Robert, C. Duboc, T. McCormac, F. Sécheresse, Dalton Trans. 8 (2006) 5141.

[44] Y.B. Liu, L.M. Duan, X.M. Yang, J.Q. Xu, J. Solid State Chem. 179 (2006) 122.

[45] Y. Xu, L.B. Nie, G.N. Zhang, Q. Chen, X.F. Zheng, Inorg. Chem. Commun. 9 (2006) 329.

[46] J. Liu, J.N. Xu, Y.B. Liu, Y.K. Lu, J.F. Song, X. Zhang, X.-B. Cui, J.Q. Xu, T.G. Wang, J. Solid State Chem. 180 (2007) 3456.

[47] W.T.A. Harrison, L. Hannoman, Angew. Chem. Int. Ed. Engl. 36 (1997) 640.

[48] G.Y. Yang, S.C. Sevov, J. Am. Chem. Soc. 121 (1999) 8389.

[49] C.N.R. Rao, S. Natarajan, S. Neeraj, J. Am. Chem. Soc. 122 (2000) 2810.

[50] M. Yuan, Y.Y. Li, E.B. Wang, Y. Lu, C.W. Hu, N.H. Hu, H.Q. Jia, J. Chem. Soc., Dalton Trans. 8 (2002) 2916.

[51] E. Burkholder, V. Golub, C.J. O'Connor, J. Zubieta, Inorg. Chem. Commun. 7 (2004) 363.